

Development 136, 1571-1581 (2009) doi:10.1242/dev.029983

Drosophila Tubulin-specific chaperone E functions at neuromuscular synapses and is required for microtubule network formation

Shan Jin^{1,2}, Luyuan Pan¹, Zhihua Liu¹, Qifu Wang¹, Zhiheng Xu¹ and Yong Q. Zhang^{1,*}

Hypoparathyroidism, mental retardation and facial dysmorphism (HRD) is a fatal developmental disease caused by mutations in tubulin-specific chaperone E (*TBCE*). A mouse *Tbce* mutation causes progressive motor neuronopathy. To dissect the functions of TBCE and the pathogenesis of HRD, we generated mutations in *Drosophila tbce*, and manipulated its expression in a tissue-specific manner. *Drosophila tbce* nulls are embryonic lethal. Tissue-specific knockdown and overexpression of *tbce* in neuromusculature resulted in disrupted and increased microtubules, respectively. Alterations in TBCE expression also affected neuromuscular synapses. Genetic analyses revealed an antagonistic interaction between TBCE and the microtubule-severing protein Spastin. Moreover, treatment of muscles with the microtubule-depolymerizing drug nocodazole implicated TBCE as a tubulin polymerizing protein. Taken together, our results demonstrate that TBCE is required for the normal development and function of neuromuscular synapses and that it promotes microtubule formation. As defective microtubules are implicated in many neurological and developmental diseases, our work on TBCE may offer novel insights into their basis.

KEY WORDS: *Drosophila*, HRD, Spastin, TBCE (CG7861), Tubulin chaperone

INTRODUCTION

Microtubules (MTs), one of the major building blocks of cells, play a crucial role in a diverse array of biological functions including cell division, cell growth and motility, intracellular transport and the maintenance of cell shape. As MTs are important in all eukaryotes, it is not surprising that defects in MTs are associated with a number of severe human diseases, including Fragile X mental retardation and autosomal dominant hereditary spastic paraplegia (AD-HSP) (Lewis and Cowan, 2002; Penagarikano et al., 2007; Reid, 1997; Roll-Mecak and Vale, 2005; Sherwood et al., 2004; Trotta et al., 2004; Zhang and Broadie, 2005). MTs are formed by polymerization of tubulin heterodimers consisting of one α - and one β -tubulin polypeptide. The formation of α - β tubulin heterodimers is mediated by a group of five tubulin chaperones, TBCA-TBCE (Tian et al., 1996) (for reviews, see Lewis et al., 1997; Nogales, 2000). TBCA and TBCD assist in the folding of β -tubulin, whereas TBCB and TBCE facilitate the folding of α -tubulin (Lewis et al., 1997; Tian et al., 2006).

A group of rare, recessive and fatal congenital diseases, collectively called hypoparathyroidism, mental retardation and facial dysmorphism (HRD), is caused by mutations in the gene encoding TBCE (Parvari et al., 2002). TBCE contains three functional domains: a glycine-rich cytoskeleton-associated protein domain (CAP-Gly) that binds α -tubulin, a series of leucine-rich repeats (LRR), and an ubiquitin-like (UBL) domain; the latter two mediate protein-protein interactions (Bartolini et al., 2005; Grynberg et al., 2003; Parvari et al., 2002). Identification of the HRD disease gene revealed a 12 bp deletion in *TBCE* that leads to the expression of a mutated TBCE protein lacking four amino acids in the CAP-Gly

domain (Parvari et al., 2002). The mutation causes lower MT density at the MT organizing center, perturbed MT polarity and decreased precipitable MT, while total tubulin remains unchanged (Parvari et al., 2002). Remarkably, overexpression of TBCE in cultured cells also results in disrupted MTs (Bhamidipati et al., 2000; Sellin et al., 2008; Tian et al., 2006). Thus, both loss-of-function mutations and overexpression of *TBCE* disrupt the MT network in mammalian systems.

Two independent studies have demonstrated that a Trp524Gly substitution at the last residue of mouse TBCE results in progressive motor neuronopathy (PMN), which has been widely used as a model for human motor neuron diseases (Bommel et al., 2002; Martin et al., 2002). Similar to what has been reported for cells from human HRD patients, the point mutation in mouse *Tbce* leads to a reduced number of MTs in axons (Bommel et al., 2002). Isolated motor neurons from mutant mice exhibit shorter axons and irregular axonal swellings (Martin et al., 2002). More specifically, axonal MTs are lost progressively from distal to proximal, which correlates with dying-back axonal degeneration in mutant mice (Schaefer et al., 2007). This demonstrates a mechanistic link between TBCE-mediated tubulin polymerization and neurodegeneration.

TBCE is well conserved across species, from yeast to human. Genetic analyses of the TBCE homolog in *S. pombe*, StolP, showed that it is essential for viability and plays a crucial role in the formation of cytoplasmic MTs and in the assembly of mitotic spindles (Grishchuk and McIntosh, 1999; Radcliffe et al., 1999). *S. cerevisiae* mutants of the *TBCE* homolog *PAC2* show increased sensitivity to the MT-depolymerizing agent benomyl (Hoyt et al., 1997). Similarly, *tbce* mutants of *Arabidopsis* have defective MTs, leading to embryonic lethality (Steinborn et al., 2002).

The *Drosophila* genome contains a TBCE ortholog, listed as CG7861 in FlyBase (<http://flybase.org>), but no studies of it have been reported. To gain a mechanistic insight into the in vivo functions of TBCE, we introduced different mutations into *Drosophila tbce*. *Drosophila tbce* nulls are embryonic lethal, indicating that it is an essential gene. We also examined the

¹Key Laboratory of Molecular and Developmental Biology, Institute of Genetics and Developmental Biology, Chinese Academy of Sciences, Beijing 100101, China.

²College of Life Sciences, Hubei University, Wuhan, Hubei 430062, China.

*Author for correspondence (e-mail: yqzhang@genetics.ac.cn)

developmental, physiological and pharmacological consequences with regard to neuromuscular synapses and MT formation when the expression of TBCE was altered specifically in neurons or muscles using the UAS-Gal4 system (Brand and Perrimon, 1993). We found that TBCE is required for the normal development and function of neuromuscular synapses and that it promotes MT formation in vivo.

MATERIALS AND METHODS

Drosophila husbandry and stocks

Flies were cultured in standard cornmeal media at 25°C, unless specified. *w¹¹¹⁸* was used as the wild-type control. Other stocks used include muscle-specific *C57-Gal4* (Budnik et al., 1996), pan-neuronal *elav-Gal4*, and deficiencies *Df(2R)ED1484* and *Df(2R)ED1482*, which remove *tbce* completely (Bloomington Stock Center). The *spastin*-null mutant *spastin^{5.75}* was from N. Sherwood (Sherwood et al., 2004), and a *UAS-spastin* line was from K. Broadie (Trotta et al., 2004). The chemical mutagen ethyl methanesulfonate (EMS)-induced nonsense mutation *Z0241* in *tbce* (see Fig. 1B) was obtained from a TILLING (targeting induced local lesions in genomes) service at Seattle (<http://tilling.fhcr.org>).

P element-mediated excision was used to generate small deletions in *tbce* following a standard protocol. The original stock *KG09112* from Bloomington has a *P* element insertion in the intergenic region between *CG14591* and *tbce* (Fig. 1B). Before mobilizing *KG09112* as mediated by *P* transposase $\Delta 2-3$, we isogenized the original stock. *w⁺* deletion lines with the *P* insertion excised either precisely (*LH198*) or imprecisely (*LH260* and *LH15*) were initially screened by PCR followed by DNA sequencing, in conjunction with immunochemical analyses to confirm the mutations at the protein level.

Production of UAS and RNAi transgenic flies

For overexpression studies, a UAS-TBCE construct was made by amplifying the full-length *tbce* cDNA from EST clone GM13256, obtained from the *Drosophila* Genomics Resource Center (<https://dgrc.cgb.indiana.edu/vectors>), and cloned into the transformation vector pUAST. For tissue-specific knockdown assays, an RNAi construct was made according to a previously described procedure (Kalidas and Smith, 2002). Specifically, a cDNA fragment from the *tbce* second exon was fused to the corresponding genomic sequence plus intron 2 as a spacer (see Fig. 1B) to make a hairpin RNAi construct targeting nucleotides 337-842 of GenBank sequence NM_136353. An independent RNAi line targeting a different sequence (nucleotides 919-1280 of NM_136353) of *tbce* was obtained from the Vienna Stock Center. Although multiple independent lines of transgenic flies carrying UAS-TBCE or RNAi were generated, here we report on UAS-TBCE and UAS-RNAi insertions on the third chromosome with apparent effect. To ensure high efficiency of overexpression or knockdown of TBCE by the UAS-Gal4 system, flies, including wild-type controls, were raised at 28°C instead of 25°C for all the assays involving the UAS and RNAi transgenic lines.

Production of monoclonal antibody against TBCE

His-tagged peptide corresponding to the N-terminal 512 amino acids of TBCE (full-length TBCE is 542 amino acids) produced in *E. coli* was used as antigen. Immunization and screening of antibody producing cells were performed according to standard procedures. Several positive clones were identified, but the antibody produced by clone 8E11 is specific for both western and immunostaining.

Behavioral analyses

The larval roll-over assay was performed largely according to published protocols (Bodily et al., 2001; Pan et al., 2008). Before the assay, larval culture and agar plates were placed at room temperature for 2 hours to acclimatize. For each assay, an individual animal was placed on a 1% agar plate and allowed to move freely for 2 minutes. The test animal was rolled over using a soft brush to a completely inverted position, indicated by the ventral midline facing up. The time that the animal took to totally right itself was recorded. Three assays were performed continuously without any resting time for each animal, and then averaged to produce one data point.

Immunochemical analyses and confocal microscopy

For western analyses, third instar larvae were dissected in PBS with all internal organs removed, followed by homogenization in 2× loading buffer. Half a fillet was used for each loading. Primary antibodies used were anti-TBCE (1:200), anti- α -tubulin (1:50,000; mAb B-5-1-2, Sigma) and anti-actin (1:50,000; mAb1501, Chemicon). The blots were detected with horseradish peroxidase (HRP)-coupled secondary antibodies using a chemiluminescent method (ECL Kit, Amersham).

Whole-mount embryos were fixed and stained with anti-FASII [1:100; Developmental Studies Hybridoma Bank (DSHB) at the University of Iowa] and BP102 antibody (1:200; DSHB) using standard procedures. For immunostaining of first instar larvae, animals were dissected and processed following an established protocol (Budnik et al., 2006). The medical adhesive Compont (Shunkang, Beijing, China) was used to glue the epidermis of larvae to Sylgard-coated coverslips. Dissection and antibody staining of third instar larvae are described elsewhere (Zhang et al., 2001). Primary antibodies used include: anti- α -tubulin (1:1000; Sigma), anti-TBCE (1:1), Texas Red-conjugated goat anti-HRP (1:50; Jackson Laboratory), anti-Futsch (1:1000; DSHB) and anti-Discs large (DLG) 4F3 (1:1000; DSHB). All primary antibodies were visualized using Alexa 488- or Cy3-conjugated goat anti-mouse IgG (1:200; Invitrogen). To examine the MT network in muscles, muscle 2 in abdominal segment A4 was analyzed as it has fewer tracheal branches to obscure the observation of MTs. Nuclei were visualized by staining with propidium iodide (PI; 1.25 μ g/ml) for 30 minutes at room temperature. Images were collected with a Leica SP5 confocal microscope and processed using Adobe Photoshop.

NMJ quantifications largely followed published procedures (Zhang et al., 2001). All images analyzed were projections from complete *z*-stacks through the entire NMJ4 of abdominal segment A3. Synaptic boutons were defined according to anti-HRP (presynaptic) and anti-DLG (postsynaptic) staining. Branches originating directly from the nerve entry point were defined as primary branches, and each higher-order branch was counted only when two or more boutons in a string could be observed. For bouton area analyses, ImageJ 3.0 (NIH) was used to define anti-HRP-stained individual boutons. The software output reports the area for each bouton automatically. At least 22 NMJ4 terminals of different genotypes were analyzed.

Futsch staining intensity relative to HRP staining at NMJ synapses was quantified largely according to Trotta et al. (Trotta et al., 2004). Staining intensities of Futsch and HRP from an entire NMJ4 terminal were digitalized automatically using ImageJ 3.0. Synaptic boutons with different Futsch staining patterns were quantified following published procedures (Packard et al., 2002; Sherwood et al., 2004). Synaptic boutons were divided into three types based on the Futsch staining pattern: (1) continuous (bundle or splayed bundle), (2) looped, and (3) diffuse (punctate) or no staining. Terminal boutons were defined as those at the ends of synaptic branches. Fourteen NMJ4 terminals from seven animals for each genotype were statistically analyzed for Futsch expression features (see Fig. 7G-I).

For quantification of tubulin staining in muscles, all images analyzed were three-dimensional projections of serial stacks through the muscle cell. The perinuclear areas were defined as the coverage that spans 10 μ m around nuclei, which were stained with PI. Tubulin staining signals within the perinuclear area from muscle 2 of abdominal segment A4 were calculated using ImageJ 3.0. The software reports the ratio of the tubulin-positive area divided by the total perinuclear area. At least four readings, one from one animal, were analyzed for each genotype.

Physiological assays

Intracellular recordings were carried out at 18°C following a conventional procedure (Jan and Jan, 1976). Specifically, wandering third instar larvae were dissected in Ca²⁺-free HL3.1 saline (Feng et al., 2004) and recorded in HL3.1 saline containing 0.25 mM Ca²⁺. Intracellular microelectrodes with a resistance of 10-20 M Ω filled with 3M KCl were used for the assay. Recordings were performed using an Axoclamp 2B amplifier (Axon Instruments) in Bridge mode. Data were filtered at 1 kHz, digitized using a Digitizer 1322A (Axon Instruments) and collected with Clampex 9.1 software (Axon Instruments). EJPs were evoked at 0.3 Hz by a suction electrode with a depolarizing pulse delivered by a Grass S48 stimulator (Astro-Grass). EJPs were recorded from muscle 6 of abdominal segment

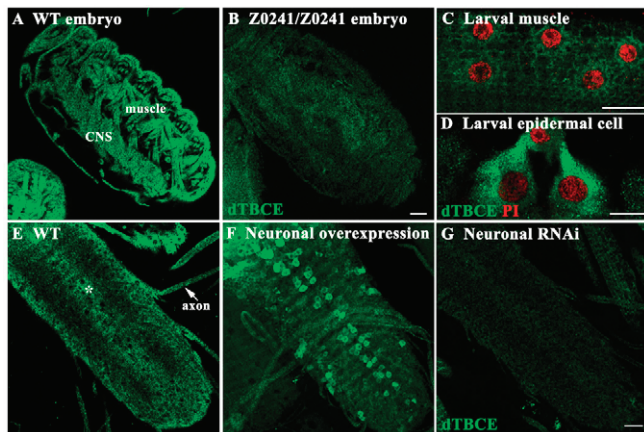


Fig. 2. TBCE is cytoplasmic and ubiquitously expressed in neuromusculature. (A,B) Wild-type (WT) and *Z0241* mutant *Drosophila* embryos stained with the 8E11 anti-TBCE monoclonal antibody. WT embryos showed specific and substantial expression of TBCE in the ventral nerve cord (CNS) and muscles (A), whereas mutant embryos showed no specific expression (B). (C,D) Immunostaining of larval muscles (C) and epidermal cells (D) showed that TBCE protein is localized in the cytoplasm and excluded from the nucleus. (E) Weak expression of TBCE was observed in the central neurons (asterisk) and peripheral axons (arrow). (F,G) Cytoplasmic TBCE in the ventral ganglion neurons was clearly seen when TBCE was pan-neuronally overexpressed using *elav-Gal4* (F), whereas no appreciable expression of TBCE was observed when RNAi was driven by *elav-Gal4* (G). Scale bars: 20 μm.

TBCE is cytoplasmic and ubiquitously expressed

Previous TBCE overexpression studies in HeLa cells detected TBCE in the cytoplasm (Bhamidipati et al., 2000; Tian et al., 2006). Mouse TBCE is enriched in motor neurons and localizes in both crude membrane and cytosolic fractions prepared from spinal cord (Schaefer et al., 2007). We investigated the expression pattern and subcellular localization of *Drosophila* TBCE using our 8E11 monoclonal antibody. The antibody detected a single band of 60 kDa, as expected from the deduced amino acid sequence (Fig. 1C). Immunostaining of embryos with the anti-TBCE antibody showed that TBCE is ubiquitously expressed, with particular enrichment in the central nervous system (CNS) and muscles (Fig. 2A). No expression was detected in *Z0241* homozygous mutants (Fig. 2B), confirming the specificity of the antibody. The expression of TBCE decreased as the animal developed from embryo to larva. In the third instar larva, weak expression with a perinuclear enrichment was observed in muscles (Fig. 2C), whereas substantial expression was observed in epidermal cells (Fig. 2D). In both cell types, TBCE was clearly cytoplasmic and excluded from the nucleus (Fig. 2C,D). Low-level expression of TBCE was also seen in the central neurons and peripheral axons of the wild-type (WT) larva (Fig. 2E). Corresponding changes in TBCE levels were observed in the central neurons of a ventral ganglion when *tbce* was overexpressed or knocked down by *elav-Gal4* (Fig. 2F,G), demonstrating the efficacy of the UAS and RNAi transgenes. Like endogenous TBCE (Fig. 2C,D), overexpressed TBCE was also cytoplasmic (Fig. 2F).

TBCE is required for microtubule formation, axonal growth and coordinated larval locomotion

Drosophila tbce nulls are embryonic lethal, with a few escapers developing to first instar larvae. To reveal the effects of TBCE on MTs, we stained mutant first instar larvae with anti- α -tubulin. The

MT network was greatly decreased, with fewer and shorter MT fibers in mutant muscle cells as compared with the dense and evenly distributed MT network in the WT (compare Fig. 3D with 3B), indicating that TBCE is required for MT formation or maintenance.

A mutated *Tbce* in mouse leads to retarded axonal growth and axonal degeneration (Bommel et al., 2002; Martin et al., 2002; Schaefer et al., 2007). To assess the role of TBCE in neuronal development, we stained stage 16 embryos with anti-FASII, which detects a set of three longitudinal axon bundles, and with BP102 antibody, which recognizes the anterior and posterior commissures and longitudinal connectives of the ventral nerve cord (VNC). As shown in Fig. 3E, anti-FASII staining of WT embryos showed three parallel longitudinal axon bundles at either side of the body. Compared with the WT, *Z0241/Df* [*Df(2R)1482* or *Df(2R)1484* removes *tbce* completely] and *LH15/Df* mutants showed longitudinal axon bundles that crossed at the midline (Fig. 3F,G). Interrupted axon bundles were also observed (Fig. 3G). Heteroallelic *Z0241/LH15* had comparable axonal defects (data not shown). WT embryos stained with BP102 antibody showed a regular ladder-like pattern of axons in the VNC (Fig. 3H). However, the regular pattern of axons was grossly disrupted in *tbce* mutants with interrupted or missing longitudinal bundles (Fig. 3I,J). The dramatic axonal defects in *tbce* nulls suggest that TBCE is required for axonal growth in *Drosophila*.

To understand the physiological functions of TBCE, we performed behavioral assays. As *tbce* nulls are embryonic lethal, we examined the behavior of larvae in which TBCE expression had been genetically altered in a tissue-specific fashion by the UAS-Gal4 system. Tissue-specific knockdown of *tbce* in neurons by *elav-Gal4* or in muscles by *C57-Gal4* produced fully developed larvae (they were late pupal lethal and fully viable, respectively) with normal rhythmic peristalsis and crawling activity (data not shown). However, a larval roll-over assay revealed obvious and profound locomotion defects when TBCE expression was altered. As a genetic control, transgenic flies of *elav-Gal4*, *C57-Gal4*, *UAS-tbce* and *UAS RNAi* without alterations in TBCE expression showed indistinguishable roll-over time from the WT (Fig. 4). However, *tbce* knockdown in neurons and muscles caused significantly slower locomotion compared with the WT, with the average roll-over time increased to 205% and 246%, respectively (Fig. 4). Similarly, neuronal and muscular overexpression of TBCE also caused a significantly compromised roll-over performance compared with the WT, with average roll-over time increased to 168% and 190%, respectively (Fig. 4). The abnormal behavior of animals with altered TBCE expression indicates that TBCE is required for the physiological function of the neuromusculature.

TBCE regulates the development of neuromuscular junction synapses

Abnormal synapses are associated with misregulated MTs (Roos et al., 2000; Sherwood et al., 2004; Trotta et al., 2004). To understand the molecular pathogenesis of HRD, we examined the development of neuromuscular junction (NMJ) synapses in flies in which *tbce* expression had been manipulated by the UAS-Gal4 system. *Drosophila* NMJ synapses are a commonly used system to examine protein function at synapses, as they are large, simple and amenable to various morphological and functional assays.

Three NMJ synapse features – synaptic branching, bouton number and average bouton area – were statistically analyzed (Fig. 5). For synaptic branching, both *elav-Gal4*-driven presynaptic and

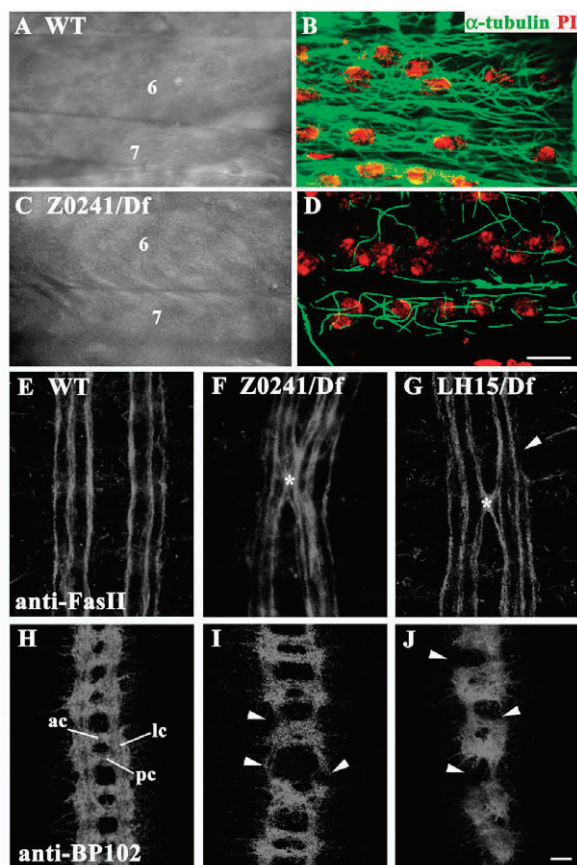


Fig. 3. TBCE is required for microtubule formation and axonal growth. (A,C) Phase-contrast images of muscles 6 and 7 of WT (A) and *Z0241/Df(2R)ED1484* mutant (C) first instar *Drosophila* larvae. (B,D) Dissected larvae were double-stained with anti- α -tubulin (green) and with propidium iodide (PI, red) to label nuclei. *tbce* mutants have a greatly reduced microtubule (MT) network and shorter MT fibers (D) compared with the WT (B). (E-J) Embryos were stained with anti-FasII, which labels three parallel longitudinal axon bundles (E-G), and with BP102 antibody, which labels the anterior and posterior commissures and longitudinal connectives of the ventral nerve cord (H-J). (E,H) WT; (F,I) *Z0241/Df*; (G,J) *LH15/Df*. Asterisks indicate midline crossing; arrowheads indicate broken longitudinal connectives. ac, anterior commissure; pc, posterior commissure; lc, longitudinal connective. Scale bars: 10 μ m.

C57-Gal4-driven postsynaptic knockdowns of *tbce* displayed a significant over-branching compared with the WT control (Fig. 5A-C,F). However, overexpression of *tbce* pre- or postsynaptically did not show the opposite phenotype to RNAi knockdown. Instead, presynaptic overexpression of TBCE resulted in normal NMJ branching, whereas postsynaptic overexpression showed mild but significant over-branching ($P=0.04$) (Fig. 5D-F). Thus, except for presynaptic overexpression of TBCE, which caused normal branching, all other manipulations of TBCE expression resulted in increased branching of NMJ synapses.

Synaptic bouton number was affected similarly to synaptic branching for the four genotypes assayed. Both the *elav-Gal4*-driven and *C57-Gal4*-driven *tbce* knockdown caused a significant increase in bouton number compared with the control (Fig. 5A-C,G). However, overexpression of TBCE by *elav-Gal4* resulted in normal bouton numbers, whereas *C57-Gal4*-driven overexpression caused a significant increase in bouton number (Fig. 5D,E,G). For synaptic

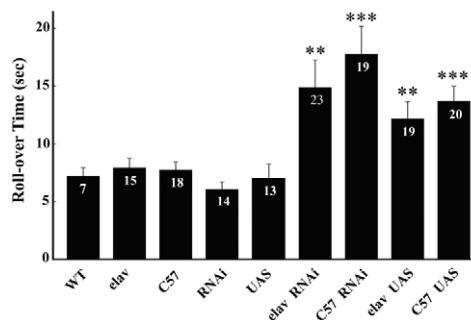


Fig. 4. Alterations in TBCE expression in neuromusculature lead to defective locomotion. The roll-over assay was performed to examine coordinated locomotion in larvae of different genotypes. Knockdown or overexpression of *tbce* specifically in muscles by *C57-Gal4*, or in neurons by *elav-Gal4*, resulted in a significant increase in roll-over time. As a control, *elav-Gal4*, *C57-Gal4*, *UAS* or *RNAi* transgenic flies without alteration of *tbce* expression showed normal roll-over, as in the WT ($P>0.05$). The number of larvae tested for each genotype is indicated. ** $P<0.01$, *** $P<0.001$; error bars indicate s.e.m.

bouton area, *C57-Gal4*-driven knockdown or overexpression of *tbce* showed significantly decreased bouton size (Fig. 5A,C,E,H). *elav-Gal4*-driven knockdown also showed decreased bouton size ($P<0.001$), but presynaptic overexpression exhibited normal bouton size (Fig. 5D,H). These NMJ phenotypes are not due to the *Gal4* driver, *UAS* or *RNAi* insertions, as these showed wild-type NMJ synapses (data not shown). In summary, quantification analyses showed that except for presynaptic overexpression of *tbce*, the remaining three manipulations of *tbce* caused increased branching number, increased bouton number and decreased bouton size at NMJ synaptic terminals. These results demonstrate that TBCE plays a crucial role in NMJ synapse development.

TBCE regulates neurotransmission at NMJ synapses

As shown above, TBCE regulates the development of NMJ synapses (Fig. 5). We then investigated whether TBCE plays a role in synaptic function. We found no change in the amplitude of excitatory junction potentials (EJPs) in animals in which TBCE had been knocked down or overexpressed postsynaptically (Fig. 6A,D-F). However, compared with the WT, both knockdown and overexpression of TBCE presynaptically elevated the EJP amplitudes significantly, by 29% and 40%, respectively (Fig. 6A-C,F). We also examined the miniature excitatory junction potentials (mEJPs), i.e. the amplitude of the response to a single vesicle release, also known as quantal size. The mEJP for the WT was 0.95 ± 0.05 mV. Knockdown and overexpression of *tbce* presynaptically increased the mEJP by 35% and 27%, respectively (Fig. 6A-C,G). The increase in EJP and mEJP was not due to *elav-Gal4*, as it displayed normal neurotransmissions (data not shown). Alterations in TBCE on the postsynaptic side caused no significant change in mEJP as compared with the WT (Fig. 6D,E,G). The quantal content – the number of vesicles released per evoked event, calculated by dividing the corrected EJP amplitude by the mEJP amplitude – was affected only when *tbce* was overexpressed presynaptically (an increase of 69%, $P<0.05$) (Fig. 6H). Presynaptic knockdown of *tbce* caused a significant increase in mEJP frequency, but other manipulations of *tbce* expression showed no significant changes (Fig. 6I).

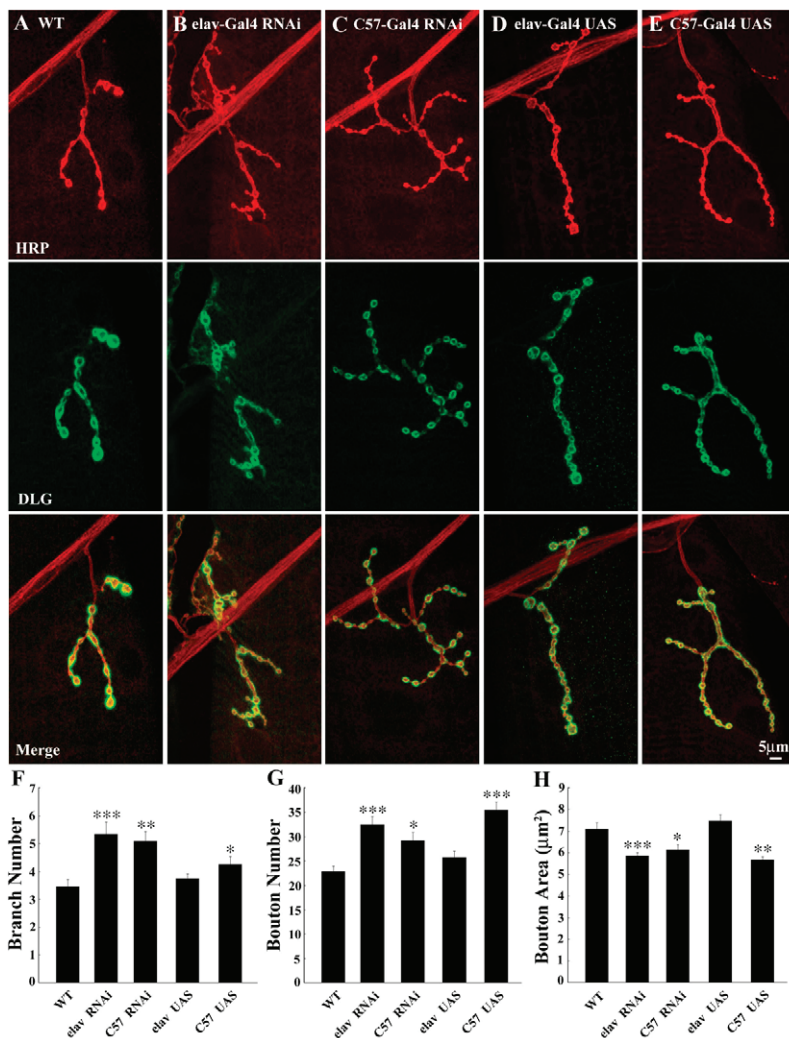


Fig. 5. TBCE regulates NMJ synapse development.

NMJs from wandering third instar *Drosophila* larvae were stained using anti-HRP (red) and anti-DLG (green) antibodies, to reveal the pre- and postsynaptic domains, respectively. Representative images of the NMJ on muscle 4 of abdominal segment A3 are shown. (A) WT control. (B) *elav-Gal4*-driven presynaptic RNAi knockdown. (C) *C57-Gal4*-driven postsynaptic RNAi knockdown. (D) *elav-Gal4*-driven overexpression of TBCE. (E) *C57-Gal4*-driven overexpression of TBCE. Scale bar: 5 µm. (F-H) Quantification of NMJ branch number (F), bouton number (G), and bouton area (H), for the different genotypes ($n \geq 22$). * $P < 0.05$, ** $P < 0.01$, *** $P < 0.001$; error bars indicate s.e.m.

In summary, altering the dosage of *tbce* on the postsynaptic side had no effect on the neurotransmission parameters we examined. But, a precisely controlled expression of *tbce* on the presynaptic side was necessary for the normal function of NMJ synapses. Taken together, these analyses demonstrate that TBCE functions presynaptically to control neurotransmission at NMJ synapses.

TBCE is required for MT formation in presynaptic terminals

A previous study revealed decreased MT density in mutant cells from HRD patients (Parvari et al., 2002). In *Tbce* mutant mice, axonal MT loss proceeds retrogradely in parallel with the axonal dying-back process (Martin et al., 2002; Schaefer et al., 2007). To investigate the effect of TBCE on MTs in the nervous system, we stained third instar larvae with antibodies against α -tubulin, Futsch (the fly ortholog of mammalian MAP1B; MTAP1B) and HRP (Fig. 7). As shown in Fig. 7B, *tbce* knockdown in presynaptic neurons resulted in obviously decreased, interrupted or even missing MTs at the distal part of the synaptic terminal detected by anti- α -tubulin staining (Fig. 7B-B'). Overexpression of *tbce*, however, led to smooth and continuous α -tubulin staining, compared with the WT (compare Fig. 7C' with 7A'). Anti-Futsch is a useful marker to reveal stabilized MTs specifically in neurons (Fig. 7D-F). Similar to the α -tubulin

staining, a much weaker and thinner staining with anti-Futsch, with weak or no staining in the terminal boutons, was observed when *tbce* was knocked down (Fig. 7E'). Statistical analyses showed that the Futsch staining intensity relative to that of HRP was significantly decreased in the knockdown and increased upon overexpression of TBCE in presynaptic neurons, as compared with the WT (Fig. 7D-F,G).

To further define the effect of TBCE on MTs, we quantified synaptic boutons based on the Futsch staining pattern. *tbce* knockdown in presynaptic neurons caused significantly decreased numbers of synaptic boutons that had organized (continuous and looped) Futsch, and increased numbers of boutons with diffuse or no Futsch signals (82.28%), as compared with the WT (23.57%) (Fig. 7H). By contrast, boutons with Futsch loops were significantly increased, and boutons with diffuse or no Futsch staining were decreased, when TBCE was overexpressed (Fig. 7H). These differences were also reflected in terminal boutons. Only 69% of terminal boutons in *tbce* knockdown animals had Futsch-positive boutons, compared with 98% in the WT, whereas TBCE overexpression showed a similar number of Futsch-positive boutons as the WT (Fig. 7I). In summary, knockdown of *tbce* in presynaptic neurons resulted in decreased MTs, whereas overexpression of *tbce* led to increased MTs in synaptic terminals.

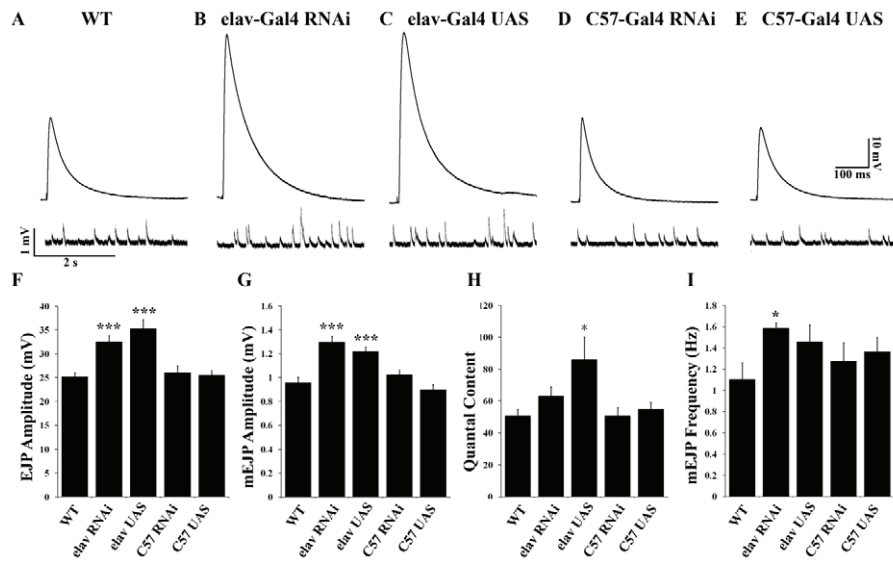


Fig. 6. Altering the presynaptic expression of *tbce* causes increased neurotransmission.

(A-E) Representative traces of excitatory junction potentials (EJPs) (upper row) and miniature excitatory junction potentials (mEJPs) (lower row) of NMJ synapses from WT (A), presynaptic RNAi (B), presynaptic overexpression (C), postsynaptic RNAi (D) and postsynaptic overexpression (E) of *tbce*.

(F-I) Quantification of EJP amplitudes (F), mEJP amplitudes (G), quantal content (H) and mEJP frequencies (I) for the different genotypes ($n \geq 9$). * $P < 0.05$, *** $P < 0.001$; error bars indicate s.e.m.

TBCE antagonizes Spastin to regulate MT formation

To better understand how TBCE affects MTs, we studied its genetic interaction with Spastin. Spastin severs the MT network in cultured cells and *Drosophila* neuromusculature (Errico et al., 2002; Roll-Mecak and Vale, 2005; Sherwood et al., 2004; Trotta et al., 2004). We first confirmed that Spastin severs MTs when it is overexpressed in muscles (see Fig. 8D) (see also Sherwood et al., 2004; Trotta et al., 2004), although no obvious abnormality in the MT network was observed in *spastin* nulls (Fig. 8E).

Compared with the thin presynaptic neuronal terminals (Fig. 7), muscle cells enabled a much higher resolution visualization of MTs (Fig. 8). In the large multi-nucleated muscle cells ($80 \times 400 \mu\text{m}$) from a third instar larva, a remarkable MT meshwork was revealed by anti- α -tubulin staining, with the highest intensity of staining around the nucleus (Fig. 8A). The intensity of perinuclear MT staining was quantified for various genotypes (see Fig. S1 in the supplementary material). Compared with the WT, overexpression of *tbce* in muscles increased the MT network dramatically, with a prominent perinuclear enrichment (Fig. 8B). Indeed, the perinuclear MTs had to be overexposed in order to see individual MT fibers in the area distal to the nucleus (Fig. 8B). Conversely, RNAi knockdown of *tbce* decreased the network, with sparser and shorter MT fibers (Fig. 8C). The decreased MT network was confirmed with an independent RNAi line from the Vienna Stock Center. We then examined the interaction between *tbce* and *spastin* in various combinations. When *tbce* and *spastin* were co-overexpressed, the resulting phenotype was similar to that of *spastin* overexpression alone (compare Fig. 8F with 8B,D). When *tbce* was knocked down while *spastin* was overexpressed, the phenotype was again more like that of *spastin* overexpression alone, with small MT fragments (compare Fig. 8G with 8C,D). The apparent *spastin* overexpression phenotype of shorter MT fragments in animals with altered *tbce* expression suggests that the function of *spastin* is dominant over that of *tbce*. When *tbce* was knocked down in a *spastin*-null background, the RNAi phenotype of sparser and shorter MT fibers was clearly ameliorated, although not completely rescued (compare Fig. 8H with 8C,E), indicating an antagonistic interaction between the two.

TBCE is acutely required for MT polymerization

To further elucidate the requirement for TBCE in MT formation, we treated dissected animals with the MT-depolymerizing drug nocodazole to disassemble the MTs completely, and then followed MT reformation after drug washout. We noticed that after mock treatment for 4 hours with a buffer containing the DMSO solvent, the MT network in muscles, especially in WT and *tbce*-overexpressing muscles, was not as dense as in the untreated cells (compare Fig. 9A,B with the corresponding Fig. 8A,B). As expected, $30 \mu\text{M}$ nocodazole treatment of WT animals for 4 hours eliminated the MT network, and only residual MT buds could be seen in muscles (compare Fig. 9Aa with 9A). Appreciable recovery of MTs, represented by denser perinuclear tubulin staining and longer MT fibers, could be detected 2 minutes after drug washout in the WT (Fig. 9Ab). By 5 minutes, near complete recovery of MTs was observed (compare Fig. 9Ac with 9A). *tbce*-overexpressing animals showed a similar pattern of MT recovery as the WT (compare Fig. 9Bb-Bd with the corresponding 9Ab-Ad). The recovery of MTs was much slower, however, when TBCE was knocked down by RNAi (compare Fig. 9Ca-Cd with the corresponding 9Aa-Ad). By 20 minutes, recovery of MTs was appreciable, but there was still a large number of MT buds or fibers that had not yet formed a MT network (Fig. 9Cd). By 1 hour after washout, the MTs had still not completely recovered (data not shown). For statistical analyses of MT recovery after the drug treatment, see Fig. S2 in the supplementary material. This experiment showed that *tbce* is acutely required for MT network formation.

DISCUSSION

Misregulated MTs are associated with human diseases such as Fragile X syndrome, hereditary spastic paraplegia and HRD. We have been using *Drosophila* as a model system to unravel the molecular pathogenesis of Fragile X syndrome (Reeve et al., 2008; Zhang et al., 2001; Zhang and Broadie, 2005), the most common form of inherited mental retardation. Fragile X mental retardation protein (FMRP, encoded by *FMR1*) plays an important role at synapses (Penagarikano et al., 2007; Zhang and Broadie, 2005). At the molecular level, the MT-associated protein MAP1B is a target of FMRP and is upregulated in *Fmr1* knockout mice and mutant flies

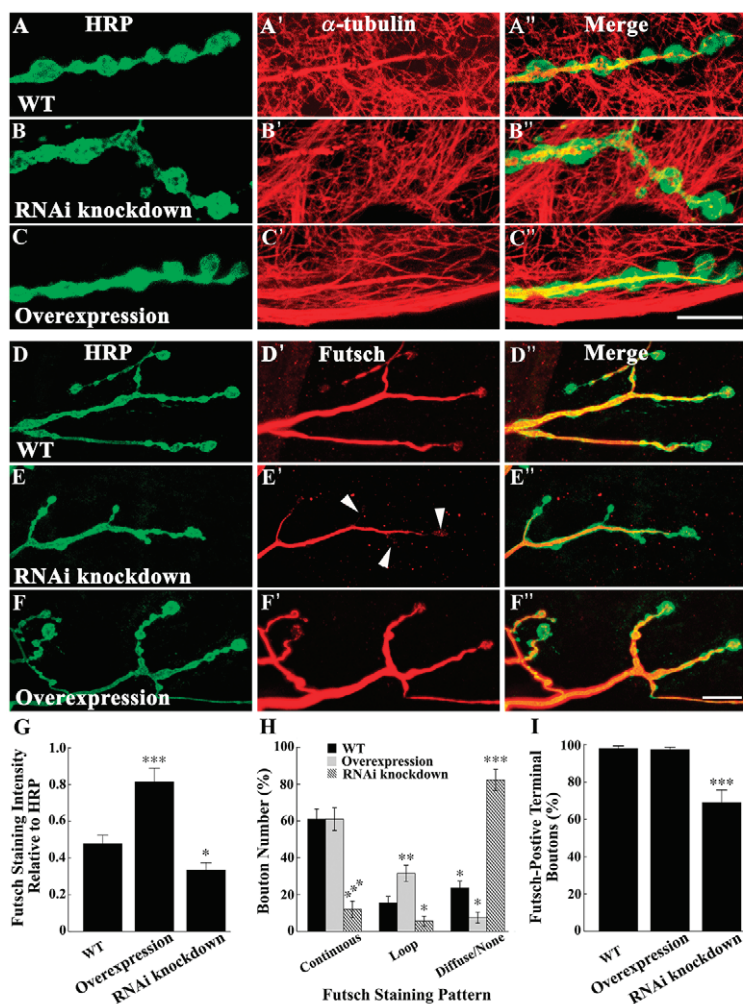


Fig. 7. Presynaptic knockdown of *tbce* results in decreased MTs in synaptic terminals. (A-C'') TBCE is required for the formation of the MT cytoskeleton. The NMJ synapses were double-stained with anti- α -tubulin (red) and anti-HRP (green). In wild-type NMJ synapses, MTs are present continuously in synaptic terminals (A-A''). When *tbce* was knocked down, the MT bundles were interrupted and not visible in the distal part of the synaptic terminal (B-B''). However, when *tbce* was overexpressed, a continuous and smooth MT cytoskeleton extending to the very tip of the terminal was observed (C-C''). (D-F'') Synaptic expression of Futsch is also regulated by TBCE. NMJ synapses were double-labeled with anti-HRP (green) and anti-Futsch (red). In presynaptic *tbce* knockdown flies, Futsch staining was dramatically decreased (E-E''), whereas overexpression of *tbce* led to an increase in Futsch staining (F-F''), as compared with the WT (D-D''). Arrowheads in E indicate terminal boutons with weak or no Futsch staining. Scale bars: 10 μ m. (G-I) Futsch staining intensity relative to that of HRP (G), the percentage of boutons exhibiting continuous, looped, or diffuse/no Futsch staining (H), and the percentage of Futsch-positive terminal boutons (I) in the different genotypes. * $P < 0.05$, ** $P < 0.01$, *** $P < 0.001$; error bars indicate s.e.m.

(Iacoangeli et al., 2008; Lu et al., 2004; Zhang et al., 2001). Since defective MTs are implicated in both Fragile X syndrome and HRD, and both diseases show mental retardation, we sought to unravel the in vivo functions of TBCE with regard to synapse development and MT formation. We provide in vivo evidence demonstrating that TBCE and the MTs that it regulates function at NMJ synapses, and that at the molecular level, TBCE is both necessary and sufficient to promote MT formation.

TBCE regulates NMJ synapse development and function

The MT cytoskeleton regulates synapse development and function, but how MT functions at synapses is poorly understood (Ruiz-Canada and Budnik, 2006). Futsch, a MT-associated protein, stabilizes MTs in presynaptic neurons, and *futsch* mutants show reduced bouton number and increased bouton size (Roos et al., 2000), whereas *spastin* mutants have the opposite phenotype of increased bouton number but decreased bouton size (Sherwood et al., 2004). Our analyses show that TBCE plays a role at synapses. Except for the presynaptic overexpression of *tbce*, all other manipulations of *tbce* at either side of the NMJ synapse caused increased branching number, increased bouton number and decreased bouton size, demonstrating that *tbce* is required for normal NMJ synapse development (Fig. 5). Given the dramatic MT alterations on both pre- and postsynaptic sides (Figs 7 and 8), the NMJ phenotypes appear subtle (Fig. 5). The seemingly

conflicting result that both overexpression and knockdown of *tbce* on the postsynaptic side led to similar phenotypes in synapse development supports an existing hypothesis that abnormal synaptic growth results from the disruption of MT dynamics, rather than from an alteration in the absolute quantity of MTs (Ruiz-Canada and Budnik, 2006).

Increased neurotransmission, reflected in both EJP and mEJP amplitude, was observed upon presynaptic alteration of *tbce* expression, whereas postsynaptic manipulations of *tbce* showed normal neurotransmission (Fig. 6). This suggests that synaptic neurotransmission is sensitive to pre- but not postsynaptic MT alteration, although postsynaptic alterations of *tbce* had a significant effect on synapse development (Fig. 5). Interestingly, both overexpression and knockdown of *tbce* on the presynaptic side led to a similar increase in both EJP and mEJP amplitude (Fig. 6). The increased EJP amplitude observed upon presynaptic alterations of TBCE might be accounted for by increased mEJP amplitude (Fig. 6). The increase in mEJP amplitude could be caused by an increase in presynaptic vesicle size, an increase in the concentration of vesicular glutamate, or an increase in postsynaptic glutamate receptor sensitivity. It is interesting to note that the mEJP is also increased in both *Fmr1*-null and *Fmr1*-overexpression NMJ synapses (Zhang et al., 2001). However, the exact mechanism by which TBCE, and other MT regulators, affect neurotransmission remains to be elucidated.

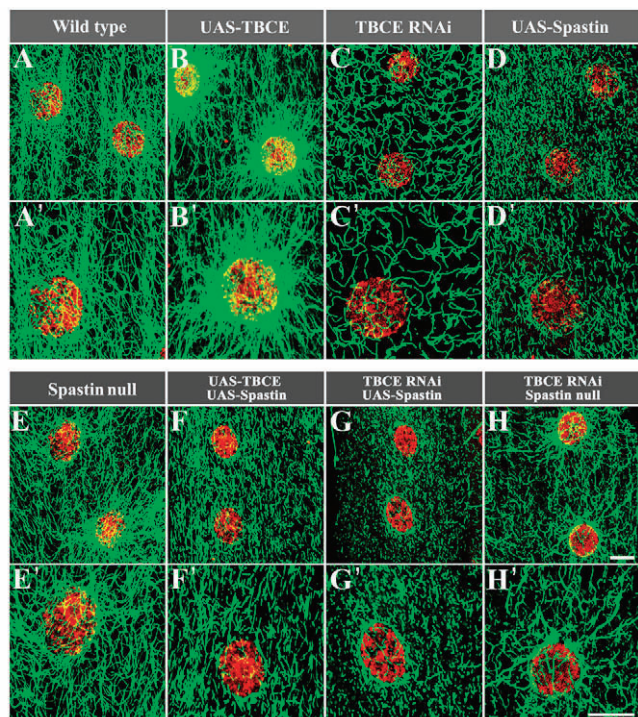


Fig. 8. *tbce* antagonizes MT-severing *spastin*. (A-H') *Drosophila* larval muscles were stained with anti- α -tubulin to show the MT network (green) and with PI to show the nucleus (red). A'-H' are higher magnification views from A-H. The MT network in the muscles is shown for the WT (A) and for *tbce* overexpression (B), *tbce* knockdown (C), *spastin* overexpression (D) and *spastin*-null (E) mutants. Co-overexpression of *tbce* and *spastin* produced a phenotype more like that of overexpression of *spastin* alone (compare F with B and D). Knockdown of *tbce* while concomitantly overexpressing *spastin* led to an enhanced form of the phenotype observed upon *spastin* overexpression alone (compare G with D). Knockdown of *tbce* in the *spastin* mutant background ameliorated the *tbce* RNAi phenotype (compare H with C and E). Scale bars: 10 μ m.

TBCE antagonizes Spastin in regulating MT dynamics

Our genetic analyses revealed an antagonistic interaction between TBCE and Spastin. TBCE promotes MT formation, whereas Spastin severs MTs. Autosomal dominant hereditary spastic paraplegia (AD-HSP) is a heterogeneous group of neurodegenerative disorders characterized by progressive and bilateral spasticity of the lower limbs, with specific degeneration of the longest axons in the CNS (Reid, 1997). Forty to fifty percent of all AD-HSP cases are caused by mutations in *spastin*. However, the MT-related pathology of human patients with *spastin* mutation has not been documented.

Overexpression of *spastin* in *Drosophila* neuromusculature (Sherwood et al., 2004; Trotta et al., 2004) and in cultured cells (Errico et al., 2002; Roll-Mecak and Vale, 2005) caused dramatically fragmented and reduced MTs. Surprisingly, morphologically normal muscles are present in patients with *spastin* mutations, although large-scale disruption of MT pathways was detected at the molecular level (Molon et al., 2004). No MT defects were reported in a mouse model in which the endogenous *spastin* is truncated (Tarrade et al., 2006). Similarly, *spastin*-null mutants of *Drosophila* show no dramatic change in MT appearance in muscles (Fig. 8E), suggesting that Spastin plays a fine-tuning role

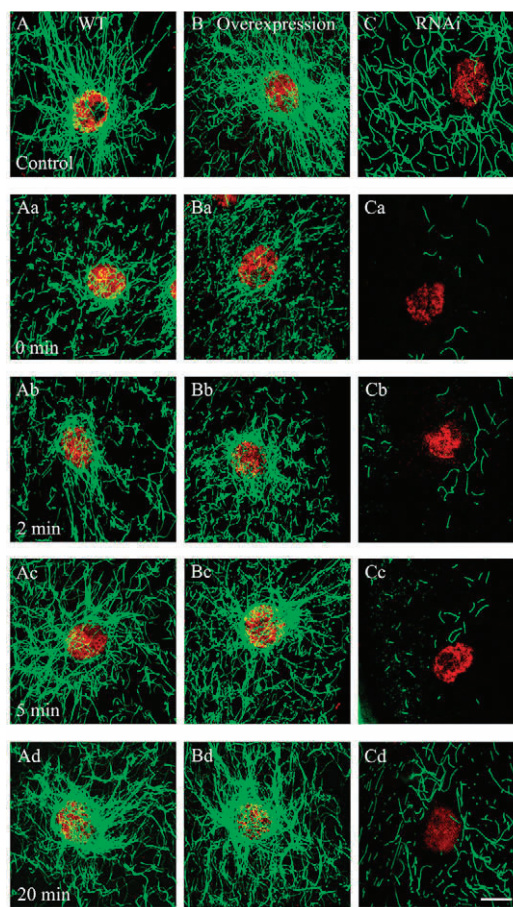


Fig. 9. TBCE is required for MT network formation. (A-Cd) Muscle MTs were examined after treatment with the MT-depolymerizing drug nocodazole. (A-Ad) WT; (B-Bd) *tbce* overexpressed; (C-Cd) *tbce* knocked down by RNAi. (A-C) Muscle MTs upon mock treatment with DMSO solvent for 4 hours. Note that the MTs in mock-treated cells of WT (A) and *tbce* overexpression (B) flies were consistently less dense than in their untreated counterparts (compare with Fig. 8A,B). (Aa-Ca) MTs in muscle cells treated with nocodazole with no washout. Ab-Cb, Ac-Cc and Ad-Cd show MTs after nocodazole washout for 2, 5 and 20 minutes, respectively. Near complete recovery of MTs by 5 minutes after washout was observed in the WT (Ac), but only weak recovery of MTs was observed in *tbce* knockdown flies (Cc). Even after 20 minutes of washout, the recovery was still not complete in *tbce* knockdown flies (Cd). MTs are labeled with anti- α -tubulin (green); nuclei are stained with PI (red). Scale bar: 10 μ m.

in MT dynamics. Indeed, *spastin* nulls are late pupal lethal with a few adult escapers, further confirming a subtle role for Spastin in MT regulation. By comparison, *tbce* nulls are embryonic lethal, whereas knockdown of *tbce* leads to a dramatically reduced MT network in *Drosophila* neuromusculature (Figs 7-9). Thus, in contrast to the nuanced role of endogenous Spastin, TBCE plays a crucial role in MT formation.

TBCE promotes MT formation

Although *Drosophila* possesses a TBCE ortholog, no previous studies of it have been reported. Our work shows for the first time that *tbce* is essential for early neuromuscular development in *Drosophila* (Fig. 3). We also provide in vivo evidence demonstrating that *Drosophila* TBCE is both required and sufficient for MT

formation (Figs 7-9), supporting early in vitro biochemical studies that showed that TBCE assists in α - β -tubulin heterodimer formation (Tian et al., 1996; Tian et al., 1997).

We found that overexpression of *tbce* produced increased MTs (Figs 7 and 8). To our knowledge, this is the first report of increased MT formation when a tubulin chaperone is overexpressed, and is contrary to reports in other systems. Overexpression of human *TBCE* in cultured cells leads to complete disruption of MTs (Bhamidipati et al., 2000; Sellin et al., 2008; Tian et al., 2006), as does overexpression of a TBCE-like protein (Bartolini et al., 2005; Keller and Lauring, 2005; Sellin et al., 2008). It was further hypothesized that the UBL domains present in TBCE and the TBCE-like protein might contribute to the degradation of tubulin via the proteasomal pathway (Bartolini et al., 2005). In addition, the overexpression of other tubulin chaperones, such as TBCD, results in a similar disruption of MTs (Bhamidipati et al., 2000; Martin et al., 2000). These in vivo data are consistent with the early in vitro observation that TBCD or TBCE in excess destroys tubulin heterodimers by sequestering the bound tubulin subunit, leading to the destabilization of the freed partner subunit (Tian et al., 1997). It is thus believed that in addition to assisting in the folding pathway, TBCE also interacts with native tubulins to disrupt α - β -tubulin heterodimers (Bhamidipati et al., 2000). The discrepancy between our overexpression result and the findings of others could have several explanations. First, the use of different experimental systems: transgenic animals in this work and cultured cells in other studies (Bhamidipati et al., 2000; Sellin et al., 2008; Tian et al., 2006). Second, different systems might have different expression levels of *tbce*, leading to varying effects on MTs. Third, *Drosophila* and human TBCE might have diverged functions. Further analyses are needed to reconcile the conflicts in the effects of TBCE overexpression in these different systems. In general, however, *tbce* mutant phenotypes are consistent in all species examined so far, from yeast to human, indicating that the function of TBCE in promoting MT formation has been well-conserved throughout evolution.

We thank K. Broadie for transgenic *UAS-spastin* flies; N. Sherwood for *spastin*^{5.75}; V. Budnik for *C57-Gal4*; the Bloomington Stock Center for fly stocks; the Developmental Studies Hybridoma Bank, University of Iowa, for antibodies; the TILLING service at Seattle for providing the nonsense mutation *Z0241*; Dr S. Y. Wang for assistance in characterizing transgenic flies; Dr F. Huang for advice on physiological assays; and Drs Z. H. Wang, C. L. Yang, X. Huang and N. Sherwood for critical reading of the manuscript. Fly transgenic work was carried out in Dr Z. H. Wang's laboratory. This work is supported by a grant from the National Science Foundation of China (NSFC) to S.J. (30871368), and grants from NSFC (30430250, 30525015), the Ministry of Science and Technology of China (2006AA02Z166, 2007CB947200) and the Chinese Academy of Sciences (KSCX1-YW-R-69) to Y.Q.Z.

Supplementary material

Supplementary material for this article is available at <http://dev.biologists.org/cgi/content/full/136/9/1571/DC1>

References

- Bartolini, F., Tian, G., Piehl, M., Cassimeris, L., Lewis, S. A. and Cowan, N. J. (2005). Identification of a novel tubulin-destabilizing protein related to the chaperone cofactor E. *J. Cell Sci.* **118**, 1197-1207.
- Bhamidipati, A., Lewis, S. A. and Cowan, N. J. (2000). ADP ribosylation factor-like protein 2 (Arl2) regulates the interaction of tubulin-folding cofactor D with native tubulin. *J. Cell Biol.* **149**, 1087-1096.
- Bodily, K. D., Morrison, C. M., Renden, R. B. and Broadie, K. (2001). A novel member of the Ig superfamily, turtle, is a CNS-specific protein required for coordinated motor control. *J. Neurosci.* **21**, 3113-3125.
- Bommel, H., Xie, G., Rossoll, W., Wiese, S., Jablonka, S., Boehm, T. and Sendtner, M. (2002). Missense mutation in the tubulin-specific chaperone E (*Tbce*) gene in the mouse mutant progressive motor neuronopathy, a model of human motoneuron disease. *J. Cell Biol.* **159**, 563-569.
- Brand, A. H. and Perrimon, N. (1993). Targeted gene expression as a means of altering cell fates and generating dominant phenotypes. *Development* **118**, 401-415.
- Budnik, V., Koh, Y. H., Guan, B., Hartmann, B., Hough, C., Woods, D. and Gorczyca, M. (1996). Regulation of synapse structure and function by the *Drosophila* tumor suppressor gene *dlg*. *Neuron* **17**, 627-640.
- Budnik, V., Gorczyca, M. and Prokop, A. (2006). Selected methods for the anatomical study of *Drosophila* embryonic and larval neuromuscular junctions. In *The Fly Neuromuscular Junction: Structure and Function*, 2nd edn (ed. V. Budnik and C. Ruiz-Canada), pp. 323-365. New York: Academic Press.
- Errico, A., Ballabio, A. and Rugarli, E. I. (2002). Spastin, the protein mutated in autosomal dominant hereditary spastic paraplegia, is involved in microtubule dynamics. *Hum. Mol. Genet.* **11**, 153-163.
- Feng, Y., Ueda, A. and Wu, C. F. (2004). A modified minimal hemolymph-like solution, HL3.1, for physiological recordings at the neuromuscular junctions of normal and mutant *Drosophila* larvae. *J. Neurogenet.* **18**, 377-402.
- Grishchuk, E. L. and McIntosh, J. R. (1999). Sto1p, a fission yeast protein similar to tubulin folding cofactor E, plays an essential role in mitotic microtubule assembly. *J. Cell Sci.* **112**, 1979-1988.
- Grynberg, M., Jaroszewski, L. and Godzik, A. (2003). Domain analysis of the tubulin cofactor system: a model for tubulin folding and dimerization. *BMC Bioinformatics* **4**, 46.
- Hoyt, M. A., Macke, J. P., Roberts, B. T. and Geiser, J. R. (1997). *Saccharomyces cerevisiae* PAC2 functions with CIN1, 2 and 4 in a pathway leading to normal microtubule stability. *Genetics* **146**, 849-857.
- Iacoangeli, A., Rozhdestvensky, T. S., Dolzhanskaya, N., Tournier, B., Schutt, J., Brosius, J., Denman, R. B., Khandjian, E. W., Kindler, S. and Tiedge, H. (2008). On BC1 RNA and the fragile X mental retardation protein. *Proc. Natl. Acad. Sci. USA* **105**, 734-739.
- Jan, L. Y. and Jan, Y. N. (1976). Properties of the larval neuromuscular junction in *Drosophila melanogaster*. *J. Physiol.* **262**, 189-214.
- Kalidas, S. and Smith, D. P. (2002). Novel genomic cDNA hybrids produce effective RNA interference in adult *Drosophila*. *Neuron* **33**, 177-184.
- Keller, C. E. and Lauring, B. P. (2005). Possible regulation of microtubules through destabilization of tubulin. *Trends Cell Biol.* **15**, 571-573.
- Lewis, S. A. and Cowan, N. J. (2002). Bad chaperone. *Nat. Med.* **8**, 1202-1203.
- Lewis, S. A., Tian, G. and Cowan, N. J. (1997). The alpha- and beta-tubulin folding pathways. *Trends Cell Biol.* **7**, 479-484.
- Lu, R., Wang, H., Liang, Z., Ku, L., O'Donnell, W. T., Li, W., Warren, S. T. and Feng, Y. (2004). The fragile X protein controls microtubule-associated protein 1B translation and microtubule stability in brain neuron development. *Proc. Natl. Acad. Sci. USA* **101**, 15201-15206.
- Martin, A. R. (1995). A further study of the statistical composition on the end-plate potential. *J. Physiol.* **130**, 114-122.
- Martin, L., Fanarraga, M. L., Aloria, K. and Zabala, J. C. (2000). Tubulin folding cofactor D is a microtubule destabilizing protein. *FEBS Lett.* **470**, 93-95.
- Martin, N., Jaubert, J., Gounon, P., Salido, E., Haese, G., Szatanik, M. and Guenet, J. L. (2002). A missense mutation in *Tbce* causes progressive motor neuronopathy in mice. *Nat. Genet.* **32**, 443-447.
- Molon, A., Di Giovanni, S., Chen, Y. W., Clarkson, P. M., Angelini, C., Pegoraro, E. and Hoffman, E. P. (2004). Large-scale disruption of microtubule pathways in morphologically normal human spastin muscle. *Neurology* **62**, 1097-1104.
- Nogales, E. (2000). Structural insights into microtubule function. *Annu. Rev. Biochem.* **69**, 277-302.
- Packard, M., Koo, E. S., Gorczyca, M., Sharpe, J., Cumberledge, S. and Budnik, V. (2002). The *Drosophila* Wnt, wingless, provides an essential signal for pre- and postsynaptic differentiation. *Cell* **111**, 319-330.
- Pan, L., Woodruff, E., 3rd, Liang, P. and Broadie, K. (2008). Mechanistic relationships between *Drosophila* fragile X mental retardation protein and metabotropic glutamate receptor A signaling. *Mol. Cell. Neurosci.* **37**, 747-760.
- Parvari, R., Hershkovitz, E., Grossman, N., Gorodischer, R., Loeyes, B., Zecic, A., Mortier, G., Gregory, S., Sharony, R., Kambouris, M. et al. (2002). Mutation of TBCE causes hypoparathyroidism-retardation-dysmorphism and autosomal recessive Kenny-Caffey syndrome. *Nat. Genet.* **32**, 448-452.
- Penagarikano, O., Mulle, J. G. and Warren, S. T. (2007). The pathophysiology of fragile x syndrome. *Annu. Rev. Genomics Hum. Genet.* **8**, 109-129.
- Radcliffe, P. A., Hirata, D., Vardy, L. and Toda, T. (1999). Functional dissection and hierarchy of tubulin-folding cofactor homologues in fission yeast. *Mol. Biol. Cell* **10**, 2987-3001.
- Reeve, S. P., Lin, X., Sahin, B. H., Jiang, F., Yao, A., Liu, Z., Zhi, H., Broadie, K., Li, W., Giangrande, A. et al. (2008). Mutational analysis establishes a critical role for the N terminus of fragile X mental retardation protein FMRP. *J. Neurosci.* **28**, 3221-3226.
- Reid, E. (1997). Pure hereditary spastic paraplegia. *J. Med. Genet.* **34**, 499-503.
- Roll-Mecak, A. and Vale, R. D. (2005). The *Drosophila* homologue of the hereditary spastic paraplegia protein, spastin, severs and disassembles microtubules. *Curr. Biol.* **15**, 650-655.

- Roos, J., Hummel, T., Ng, N., Klambt, C. and Davis, G. W. (2000). Drosophila Futsch regulates synaptic microtubule organization and is necessary for synaptic growth. *Neuron* **26**, 371-382.
- Ruiz-Canada, C. and Budnik, V. (2006). Synaptic cytoskeleton at the neuromuscular junction. *Int. Rev. Neurobiol.* **75**, 217-236.
- Schaefer, M. K., Schmalbruch, H., Buhler, E., Lopez, C., Martin, N., Guenet, J. L. and Haase, G. (2007). Progressive motor neuronopathy: a critical role of the tubulin chaperone TBCE in axonal tubulin routing from the Golgi apparatus. *J. Neurosci.* **27**, 8779-8789.
- Sellin, M. E., Holmfeldt, P., Stenmark, S. and Gullberg, M. (2008). Op18/Stathmin counteracts the activity of overexpressed tubulin-disrupting proteins in a human leukemia cell line. *Exp. Cell Res.* **314**, 1367-1377.
- Sherwood, N. T., Sun, Q., Xue, M., Zhang, B. and Zinn, K. (2004). Drosophila spastin regulates synaptic microtubule networks and is required for normal motor function. *PLoS Biol.* **2**, e429.
- Steinborn, K., Maulbetsch, C., Priester, B., Trautmann, S., Pacher, T., Geiges, B., Kuttner, F., Lepiniec, L., Stierhof, Y. D., Schwarz, H. et al. (2002). The Arabidopsis PILZ group genes encode tubulin-folding cofactor orthologs required for cell division but not cell growth. *Genes Dev.* **16**, 959-971.
- Tarrade, A., Fassier, C., Courageot, S., Charvin, D., Vitte, J., Peris, L., Thorel, A., Mouisel, E., Fonknechten, N., Roblot, N. et al. (2006). A mutation of spastin is responsible for swellings and impairment of transport in a region of axon characterized by changes in microtubule composition. *Hum. Mol. Genet.* **15**, 3544-3558.
- Tian, G., Huang, Y., Rommelaere, H., Vandekerckhove, J., Ampe, C. and Cowan, N. J. (1996). Pathway leading to correctly folded beta-tubulin. *Cell* **86**, 287-296.
- Tian, G., Lewis, S. A., Feierbach, B., Stearns, T., Rommelaere, H., Ampe, C. and Cowan, N. J. (1997). Tubulin subunits exist in an activated conformational state generated and maintained by protein cofactors. *J. Cell Biol.* **138**, 821-832.
- Tian, G., Huang, M. C., Parvari, R., Diaz, G. A. and Cowan, N. J. (2006). Cryptic out-of-frame translational initiation of TBCE rescues tubulin formation in compound heterozygous HRD. *Proc. Natl. Acad. Sci. USA* **103**, 13491-13496.
- Trotta, N., Orso, G., Rossetto, M. G., Daga, A. and Broadie, K. (2004). The hereditary spastic paraplegia gene, spastin, regulates microtubule stability to modulate synaptic structure and function. *Curr. Biol.* **14**, 1135-1147.
- Zhang, Y. Q. and Broadie, K. (2005). Fathoming fragile X in fruit flies. *Trends Genet.* **21**, 37-45.
- Zhang, Y. Q., Bailey, A. M., Matthies, H. J., Renden, R. B., Smith, M. A., Speese, S. D., Rubin, G. M. and Broadie, K. (2001). Drosophila fragile X-related gene regulates the MAP1B homolog Futsch to control synaptic structure and function. *Cell* **107**, 591-603.